Molecules and Cells

Plasma Membrane Localized GCaMP-MS4A12 by Orai1 Co-Expression Shows Thapsigargin- and Ca^{2+}-Dependent Fluorescence Increases

Jung Woo Han[1,6], Woon Heo[1,6], Donghyuk Lee[1], Choeun Kang[1], Hye-Yeon Kim[1], Ikhyun Jun[3], Insuk So[4], Hyuk Hur[5], Min Goo Lee[1], Minkyu Jung[2,*], and Joo Young Kim[1,*]

[1]Department of Pharmacology and Brain Korea 21 Plus Project for Medical Science, Yonsei University College of Medicine, Seoul 03080, Korea, [2]Division of Medical Oncology, Department of Internal Medicine, Yonsei University College of Medicine, Seoul 03080, Korea, [3]The Institute of Vision Research, Department of Ophthalmology, Yonsei University College of Medicine, Seoul 03722, Korea, [4]Department of Physiology, Seoul National University College of Medicine, Seoul 03080, Korea, [5]Department of Surgery, Yonsei University College of Medicine, Seoul 03080, Korea, [6]These authors contributed equally to this work.
*Correspondence: minkjung@yuhs.ac (MJ); jooyoungkim@yuhs.ac (JYK)
https://doi.org/10.14348/molcells.2021.2031
www.molcells.org

Uniquely expressed in the colon, MS4A12 exhibits store-operated Ca^{2+} entry (SOCE) activity. However, compared to MS4A1 (CD20), a Ca^{2+} channel and ideal target for successful leukaemia immunotherapy, MS4A12 has rarely been studied. In this study, we investigated the involvement of MS4A12 in Ca^{2+} influx and expression changes in MS4A12 in human colonic malignancy. Fluorescence of GCaMP-fused MS4A12 (GCaMP-M12) was evaluated to analyse MS4A12 activity in Ca^{2+} influx. Plasma membrane expression of GCaMP-M12 was achieved by homo- or hetero-complex formation with no-tagged MS4A12 (nt-M12) or Orai1, respectively. GCaMP-M12 fluorescence in plasma membrane increased only after thapsigargin-induced depletion of endoplasmic reticulum Ca^{2+} stores, and this fluorescence was inhibited by typical SOCE inhibitors and siRNA for Orai1. Furthermore, GCaMP-MS4A12 and Orai1 co-transfection elicited greater plasma membrane fluorescence than GCaMP-M12 co-transfected with nt-M12. Interestingly, the fluorescence of GCaMP-M12 was decreased by STIM1 over-expression, while increased by siRNA for STIM1 in the presence of thapsigargin and extracellular Ca^{2+}. Moreover, immunoprecipitation assay revealed that Orai1 co-expression decreased protein interactions between MS4A12 and STIM1. In human colon tissue, MS4A12 was expressed in the apical region of the colonic epithelium, although its expression was dramatically decreased in colon cancer tissues. In conclusion, we propose that MS4A12 contributes to SOCE through complex formation with Orai1, but does not cooperate with STIM1. Additionally, we discovered that MS4A12 is expressed in the apical membrane of the colonic epithelium and that its expression is decreased with cancer progression.

Keywords: colon cancer, GCaMP, MS4A12, Orai1, STIM1, store-operated Ca^{2+} entry

INTRODUCTION

The MS4A (membrane-spanning 4-domain family, subfamily A) gene family contains 18 members in humans (Liang and Tedder, 2001; Zuccolo et al., 2010), and their encoded proteins show tissue-specific expression (Liang and Tedder, 2001; Zuccolo et al., 2010; 2013). CD20 (MS4A1) is specifically expressed only in B cells and is a highly selective cancer marker

Received 27 January, 2020; revised 4 March, 2021; accepted 10 March, 2021; published online 23 April, 2021

eISSN: 0219-1032

for B cell lymphoma (Herter et al., 2013; Reff et al., 1994). Ca^{2+} influx of CD20 is activated by the binding of anti-CD20 monoclonal antibody (mAb) (Beers et al., 2010; Bubien et al., 1993), which is unique as a successful surface target of mAbs (Walshe et al., 2008). These features have enabled the production of blockbuster antibodies, anti-CD20 antibodies, which have greatly contributed to the success of the biopharmaceutical industry (Rogers et al., 2014). Additionally, CD20 has been shown to have store-operated Ca^{2+} influx activity (Li et al., 2003; Vacher et al., 2015). As an analogue to CD20, the MS4A family member MS4A12, a colon-specific membrane protein, has also been found to exhibit tissue-specific expression and store-operated Ca^{2+} influx activity (Koslowski et al., 2008). However, characteristics of the Ca^{2+} channel activity of MS4A12 are unclear, and the potential of MS4A12 as a colon cancer marker is controversial.

Store-operated Ca^{2+} entry (SOCE) is a major Ca^{2+} entry pathway in the epithelia (Prakriya and Lewis, 2015; Sobradillo et al., 2014; Villalobos et al., 2017; Yuan et al., 2007). Among ion channels, SOCE channels have unique biophysical properties and regulation modes. The core uniqueness is regulation by STIM protein, the only known endoplasmic reticulum (ER) Ca^{2+} sensor until now (Prakriya and Lewis, 2015). Orai channels are representative SOCE channels regulated by STIM protein, the only known ER Ca^{2+} sensor identified to date (Prakriya and Lewis, 2015). STIM1 is located in the ER membrane and senses Ca^{2+} contents in the ER (Kim and Muallem, 2011; Prakriya and Lewis, 2015; Yuan et al., 2007). Once activated by Ca^{2+} store depletion, STIM1 proteins undergo conformational changes in their EF domain and then oligomerize and accumulate in puncta near the plasma membrane to gate the Orai1 channel (Feske et al., 2006; Wang et al., 2010). Other proteins also play a key role in SOCE channels that historically have SOC channel activity, such as TRPC1. Dynamic assembly of a TRPC1-STIM1-Orai1 ternary complex is involved in activation of Ca^{2+} entry, and this is a common molecular basis for SOC and CRAC channels (Ong et al., 2007; Sabourin et al., 2015). On the other hand, the pore component of L-type Ca^{2+} channel $Ca_V1.2$ is inhibited by over-expression of STIM1 (Park et al., 2010; Wang et al., 2010), and Orai1 increases the proximity of STIM1 to $Ca_V1.2$ (Wang et al., 2010). Reportedly, over-expression of MS4A12 increased Ca^{2+} permeability via thapsigargin, and the observed permeability decreased when MS4A12 expression was knock-downed by siRNA (Koslowski et al., 2008). However, MS4A12 has not been investigated as an SOCE channel regulated by Orai1 and STIM1.

Tumour cells exhibit distinct and acquired traits that are relevant to or influenced by changes in Ca^{2+} handling (Monteith et al., 2007; Parekh, 2010; Roderick and Cook, 2008). MS4A12 was first reported to show increased expression in patients with colon cancer (Koslowski et al., 2008). However, recent reports have indicated that MS4A12 is predominantly expressed in normal colon tissues and tends to show decreased expression when transformed into cancerous tissues (Dalerba et al., 2011; Drew et al., 2014; Roberts et al., 2015). Although the direction of changes in expression during cancer progression is unclear, MS4A12 is a promising colon cancer marker for predicting both cancer diagnosis and progression (Dalerba et al., 2011; Drew et al., 2014; Koslowski et al., 2008).

GCaMP fluorescence proteins are robust tools with which to monitor Ca^{2+} concentrations nearby ion channels (Akerboom et al., 2013; Ko et al., 2017; Nguyen et al., 2020). Indeed, multiple gating states and oscillation of Orai1 has been documented by genetically encoded Ca^{2+}-indicators for optical imaging fused to the N-terminal of Orai1 protein (Dynes et al., 2016), and lysosomal Ca^{2+} efflux has been successfully measured by GCaMP3-tagged TRPML1 (Shen et al., 2012). In this study, we evaluated SOCE activity for MS4A12 based on Orai1 and STIM1 interactions. We used GCaMP6s fused with MS4A12 to measure Ca^{2+} influx near MS4A12 and to test hetero-complex formation with Orai1. Additionally, expression changes of MS4A12, as well as Orai1 and STIM1, were observed in normal and cancer tissues from the human colon.

MATERIALS AND METHODS

Clones, cell lines, materials, and human colon samples

pCMV-SPORT6-MS4A12 clones (long isotype of hMS4A12) were purchased from Korea Human Gene Bank (hMU004204), and 3X flag-MS4A12 was sub-cloned into pCMV5 vectors using *Not*I/*Bam*HI site. pLenti6.3-GCaMP6s-MS4A12 was produced using *Bam*HI/*Spe*I sites for GCaMP6s and *Spe*I/*Xho*I sites for MS4A12 into pLenti6.3 vectors. C-term truncated MS4A12 was produced by insertion of a stop codon by mutagenesis at the 224th amino acid. Truncation mutants of STIM1 and $STIM1^{D76A}$ were described in a previous study (Yuan et al., 2007). Flag-Orai1 was kindly provided by Shmuel Muallem. Thapsigargin (T9033), 2-APB (D9754), and BTP2 (YM-58483) were purchased from Sigma (USA). Anti-MS4A12 antibody (HPA057657) and anti-flag (9E10) antibody were purchased in Sigma. Anti-myc antibody (2276s), anti-GOK/STIM1 antibody (610954), anti-Orai1 antibody (ACC-062), and ZO-1 antibody (ab190085) were purchased from Cell Signaling Technology (USA), BD Bioscience (USA), Alomone (Israel), and Abcam (UK), respectively. Aldolase A (N-15, sc-12059; Santa Cruz Biotechnology, USA) and β-actin (sc-1616; Santa Cruz Biotechnology) were used, and anti-mouse, anti-rabbit, or anti-goat IgG conjugated with Alexa Fluor 488, 563 (Invitrogen, USA) was utilized as secondary antibody. Anti-mouse, anti-rabbit, or anti-goat IgG conjugated with HRP was purchased form Thermo Fisher Scientific (USA). Plasmids were transiently transfected into HEK293 cells using Lipofectamine 2000 (Invitrogen) and T84 cells using ExGen 500 (Thermo Fisher Scientific). siRNA was transfected with RNAimax (Invitrogen). HEK293, A549, and CaCo2 cells were maintained in DMEM-High Glucose (Invitrogen). T84 cells were maintained in a 1:1 mixture of Ham's F-12 medium and DMEM (Invitrogen). H508 and HT29 cells were maintained in RPMI1640. All media were supplemented with 10% fetal bovine serum (Invitrogen), penicillin (50 IU/ml), and streptomycin (50 μg/ml). The experiments using human colon and cancer tissue samples were approved by the Institutional Review Board of Severance Hospital, Yonsei University College of Medicine, Seoul, Korea (IRB protocols No. 4-2014-0349). Normal tissues were obtained from tumor margins under

inspection by an oncology surgeon. All subjects provided written informed consent, and their clinicopathologic information are outlined in Supplementary Table S1.

Plasma expression of GCaMP-MS4A12

HEK cells were transfected with GCaMP-MS4A12 alone and GCaMP-MS4A12 with untagged MS4A12 or Flag tagged Orai1 (plasmid 1:1 ratio) using Lipofectamine 2000, and were grown on glass coverslips. After growing for 36 h, the cells were stimulated with 1 μM thapsigargin in 5 mM Ca^{2+} regular solution for 5 min. Then, cells on coverslips were fixed with 4% paraformaldehyde in phosphate-buffered saline and mounted on slide glass. Images were obtained with a Zeiss LSM 780 confocal microscope (Zeiss, Germany).

Ca^{2+} influx measurement using GCaMP6s-MS4A12

No-tagged MS4A12 (nt-M12) and GCaMP-MS4A12 plasmids were mixed at a 1:1 ratio and then transfected into HEK293 cells grown on coverslips. In case of Orai-GCaMP-MS4A12 hetero complex, flag-tagged Orai1 was used instead of nt-M12. At 48 h after transfection, changes in GCaMP fluorescence were assessed using a Zeiss 780 confocal microscope (Zeiss). siRNA of Orai1 and STIM1 was also transfected 1 day before MS4A12 transfection. During fluorescence measurements, cells were continually perfused with a Ca^{2+} free regular solution (37°C) containing 150 mM NaCl, 5 mM KCl, 1 mM $MgCl_2$, 10 mM glucose, and 10 mM HEPES at pH 7.4 with NaOH. Thapsigargin of 5 μM was used for stimulation and store depletion, after which 5 mM Ca^{2+} regular solution was perfused to visualize Ca^{2+} influx-induced fluorescence of GCaMP-MS4A12. To inhibit SOCE mediated Ca^{2+} influx, 5 μM 2-aminoethoxydiphenyl borate (2-APB) was treated during the measurement, and 500 nM BTP2 was pre-treated 5 min before starting the measurement. Ca^{2+} influx activity was calculated according to changes in GCaMP6s fluorescence (ΔF) at each time point over basal fluorescence (F_0; $\Delta F/F_0$). Averages $\Delta F/F_0$ of all measurements were obtained from more than three independent experiments (each comprising analyses of 4-20 cells).

Immunoprecipitation and Western blot analysis

For immunoprecipitation assay, HEK293 cells transfected with appropriate plasmid were lysed with sonication in lysis buffer (150 mM NaCl, 5 mM Na-EDTA, 10% glycerol, 20 mM Tris-HCl [pH 8.0], 0.5% Triton X-100, and proteinase inhibitors [Complete; Roche Applied Science, USA]). To capture the protein, appropriate antibody was incubated for more than 4 h, after which protein A/G beads were added to capture antibody bound protein complex. Beads were washed with 400 μl of lysis buffer four times, and 2× sample buffer was used to elute whole protein complexes. For Western blot analysis, cells were lysed in lysis buffer, and lysates were separated on 4% to 12% pre-made gradient sodium dodecyl sulfate-polyacrylamide electrophoresis gels (Koma Biotech, Korea) and transferred to membranes. For tissue experiments, human colon and cancer tissue were homogenized with lysis buffer after chopping them into small pieces. Appropriate antibodies were used to detect the proteins, and HRP-conjugated secondary antibody and ECL solution (Amersham Bioscience, UK) were used for detection by chemi-luminescence. Quantification of band intensity was performed using MultiGauge software (Fujifilm, Japan).

Reverse transcription polymerase chain reaction

Total RNA was extracted using TRIzol reagent (Invitrogen), and an equal amount of RNA from each sample was reverse-transcribed to cDNA using Superior Script II Reverse transcriptase (Enzynomics, Korea). The cDNA was amplified with specific primers and a Taq polymerase (2X TOPsimple Premix; Enzynomics). The polymerase chain reaction (PCR) primer sequences were as follows: hMS4A12 sense, ACA TTG CCC TGG GGG GTC TTC T; hMS4A12 antisense, CCA GAA ATG GCA GCA AAG AGG CT (205 bp); hSTIM1 sense, GGAAGACCTCAATTACCATGAC; hSTIM1 antisense, GCTCCTTAGAGTAACGG TTCTG (440 bp); hOrai1 sense, ACC TGC ATC CTG CCC AAC ATC; hOrai1 antisense, GCC CAG GCC AGC TCG ATG TG (107 bp); β actin-sense, GAC CCA GAT CAT GTT TGA GAC C; β-actin antisense, GGC CAT CTC CTG CTC GAA GTC; 18s ribosome sense, GTGGAGC-GATTTGTCTGGTT; and 18s ribosome anti-sense, CGCTGAG-CCAGTCAGTGTAG (199 bp).

Statistical analysis

Data are presented as the mean ± SEM. Statistical analysis was performed with Student's *t*-tests, ANOVA, followed by Tukey's multiple comparison, or one-way ANOVA using GraphPad Prism software (ver. 5.0; GraphPad Software, USA), as appropriate. *P* values ≤ 0.05 were considered statistically significant.

RESULTS

Characteristics of MS4A12 as a store-operated Ca^{2+} influx channel

To measure Ca^{2+} influx near MS4A12, GCaMP-MS4A12 (GCaMP-M12) was constructed by fusing MS4A12 with the GCaMP6s Ca^{2+} indicator, which fluoresces in response to a short-term Ca^{2+} concentration increase near MS4A12. However, GCaMP-M12 did not reach the cell membrane, likely due to the high solubility of GCaMP. HEK cells expressing GCaMP-M12 alone showed fluorescence throughout the cytosol when stimulated with thapsigargin in 5 mM Ca^{2+} solution (Fig. 1A). This problem was overcome by co-expressing GCaMP-M12 with nt-M12 at a 1:1 DNA transfecting ratio: GCaMP-M12 co-transfected with nt-M12 showed plasma membrane localization in the same thapsigargin condition (Fig. 1B). Successful plasma membrane localization proved that GCaMP-M12 complexed with nt-M12. Next, we evaluated the pharmacological characteristics of MS4A12 store-dependent Ca^{2+} influx using plasma membrane localized GCaMP-M12. First, we confirmed the spontaneous Ca^{2+} influx of MS4A12 (Fig. 1C). When 5 mM Ca^{2+} was perfused without stimulation, we observed no fluorescence increases in GCaMP-M12. However, when cells were stimulated with a store-depleting condition (5 μM thapsigargin for 5 min in the 5 mM Ca^{2+} extracellular solution), the fluorescence of GCaMP-M12 very rapidly and greatly increased (Fig. 1D, Supplementary Movie S1). Additionally, the increased fluo-

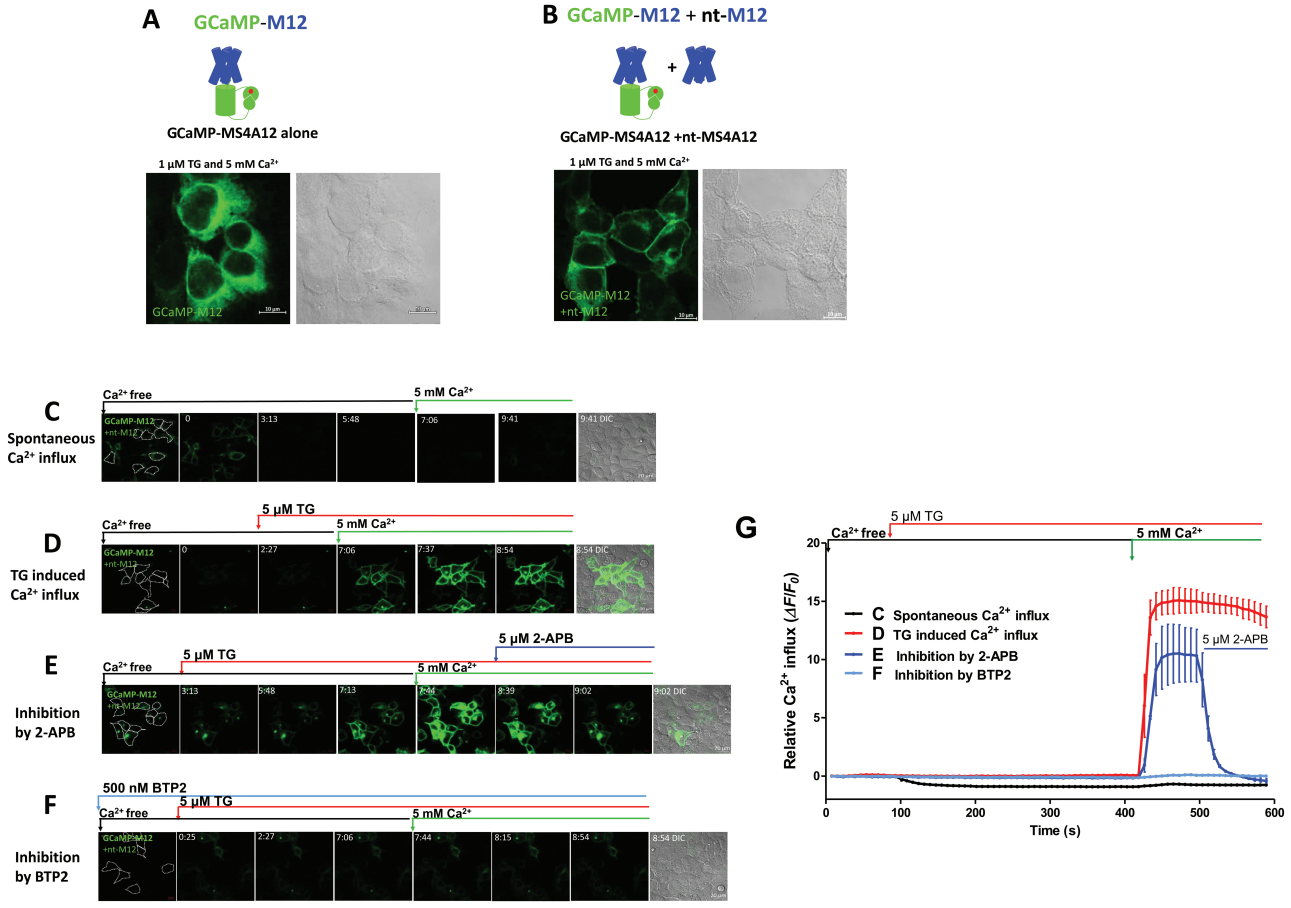

Fig. 1. GCaMP-M12 complexes with nt-M12 localized in plasma membrane, and its fluorescence is dependent on store-operated Ca^{2+} influx. (A and B) Localization of GCaMP-M12 in HEK cells upon confocal microscopy. The transmembrane domain of MS4A12 is indicated by blue rods, and GCaMP and Ca^{2+} are indicated by green and red dots, respectively. GCaMP-M12 fluorescence after treatment with 1 μM thapsigargin (TG) and extracellular 5 mM Ca^{2+} (left) and cell boundaries (differential interference contrast [DIC] image, right) were observed. Cytosolic localization of GCaMP-M12 expressed alone (A) or co-expressed with nt-M12 (B). Scale bars = 10 μm. (C-G) Fluorescence of GCaMP-M12 (green) to detect Ca^{2+} influx nearby MS4A12. Fluorescence changes in GCaMP6s (ΔF at each time point over basal fluorescence [F_0; $\Delta F/F_0$]) were traced. Average $\Delta F/F_0$ of all measurements was obtained from three independent experiments (each analysing 4-20 cells). The first and last images in each row show the before and last scene of recording, respectively. The dotted outlined cell in the first image indicates cells expressing GCaMP-M12, and the last scene image was merged with the transmission image (bar, 20 μm) to show the state of cell fluorescence. (C) Spontaneous Ca^{2+} influx when extracellular 5 mM Ca^{2+} was applied without any stimulation. (D) To induce store depletion, 5 μM thapsigargin was added, and 5 mM Ca^{2+} was extracellularly added to allow Ca^{2+} influx. No changes were observed in most cells upon thapsigargin treatment, after which 5 mM Ca^{2+} evoked increased GCaMP-M12 fluorescence. (E) 5 μM 2-APB was added to test whether the increased 5 mM Ca^{2+} with thapsigargin evoked Ca^{2+} influx was blocked. (F) 500 nM BTP2 was pre-incubated to block Ca^{2+} influx through Orai1 before performing B. (G) A summary of Ca^{2+} influx activity in (C-F).

rescence of GCaMP-M12 by store-depleting condition was inhibited by 2 mM 2-APB (Fig. 1E, Supplementary Movie S2). Furthermore, pre-treatment with 500 nM of BTP2 (Fig. 1F) completely blocked any florescence increases in the store-depleting condition.

Both the robust increase in GCaMP-M12 fluorescence under the thapsigargin and external 5 mM Ca^{2+} condition and the lack of fluorescence changes upon thapsigargin-induced internal Ca^{2+} efflux clearly demonstrated that the increased fluorescence of GCaMP-M12 occurred as a result of increased Ca^{2+} concentrations near GCaMP-M12 or increased Ca^{2+} influx through MS4A12 in plasma membrane. Accordingly, thapsigargin-dependent Ca^{2+} influx and its blockade by typical SOCE inhibitors revealed that the complex of GCaMP-M12 with nt-M12 monitors or functions as a store-operated Ca^{2+} influx pore.

Orai1 co-expression increases and Orai1 knockdown decreases thapsigargin-induced increases in GCaMP-M12 fluorescence

Measuring Ca^{2+} influx in Fura2-AM loaded HEK cells, we noted that over-expression of MS4A12 elicited increased thapsigargin-activated Ca^{2+} influx, which was further increased by STIM1 co-expression (Supplementary Fig. S1).

However, since the magnitude thereof was much smaller than STIM1 effects on Orai1, we presumed that the reason why MS4A12 showed characteristics of SOCE might be that MS4A12 could hetero-complex with Orai1. Also, STIM1 could control Orai1 gating, resulting in Ca^{2+} influx through the hetero-complex of MS4A12 and Orai1. To investigate

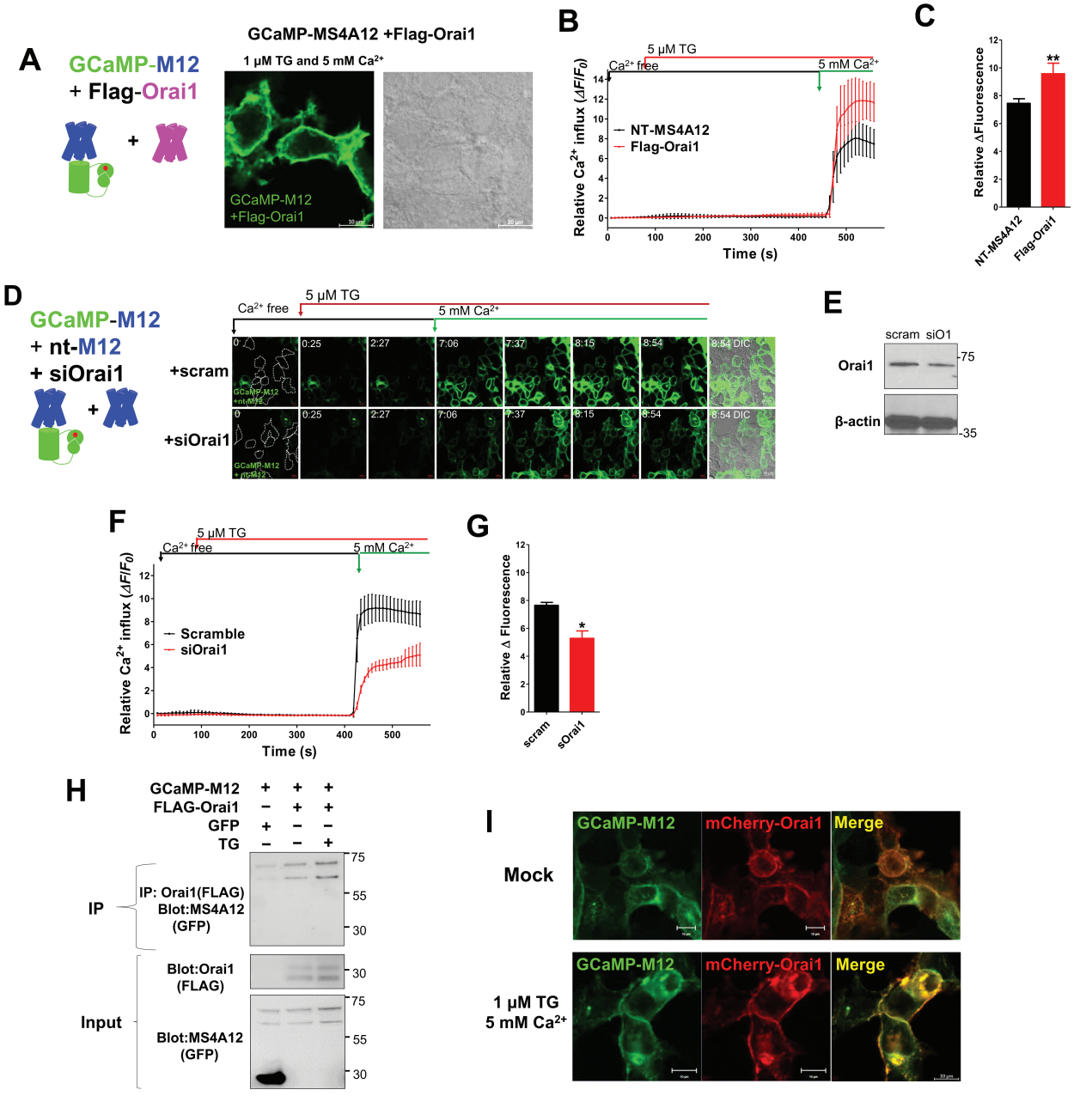

Fig. 2. Orai1 knockdown decreases, while co-expression with Orai1 increases, thapsigargin (TG)- and Ca^{2+}-dependent increases in GCaMP-M12 fluorescence. (A) Plasma membrane localization of GCaMP-M12 by co-expression with Orai1, similar to that by co-expression with nt-M12. (B and C) Thapsigargin- and Ca^{2+}-dependent fluorescence changes in GCaMP-M12 under Orai1-co-expression. (B) Thapsigargin- and Ca^{2+}-dependent fluorescence changes in GCaMP-M12 co-expressed with Flag-Orai1 and summary in (C). $**P \leq 0.01$. (D-G) Thapsigargin- and Ca^{2+}-dependent fluorescence changes in GCaMP-M12 upon Orai1 knockdown (co-expressed with nt-M12). Images of each indicated time point (D) and fluorescence changes (F) for thapsigargin- and Ca^{2+}-dependent GCaMP-M12 co-transfected with nt-MS4A12 in scramble and siOrai1-transfected cells. Summary is in (G). $*P \leq 0.05$. siRNA efficiency of Orai1 protein was confirmed by Western blot with Orai1-specific antibody (E). (H) Immunoprecipitation assay to observe protein-protein interactions for MS4A12 and Orai1. Flag and GFP antibodies were used to detect Orai1 and MS4A12, respectively. Anti-Flag antibody for Orai1 was used in immunoprecipitation for GCaMP-M12. (I) Co-localization of GCaMP-M12 and mCherry-Orai1 observed by live cell imaging in normal and thapsigargin-stimulated conditions. Scale bars = 10 μm.

the role of Orai1 in the SOCE-like behaviour of MS4A12, we observed the plasma membrane expression of GCaMP-M12 co-transfected with Flag-tagged Orai1 in its N-terminal (Flag-Orai1). As when co-expressed with nt-M12 (Figs. 1A and 1B), the fluorescence of GCaMP-M12 was observed at the plasma membrane when co-expressed with Flag-Orai1, implying that GCaMP-M12 complexes with Flag-Orai1 (Fig. 2A). Next, we compared changes in fluorescence upon thapsigargin-induced Ca^{2+} influx between GCaMP-M12 with nt-M12 and GCaMP-M12 with Flag-Orai1. Interestingly, the relative fluorescence changes were significantly higher for GCaMP-M12 co-transfected with Flag-Orai1 than for GCaMP-M12 co-transfected with nt-M12 (Figs. 2B and 2C). Additionally, we examined thapsigargin-induced Ca^{2+} influx-mediated fluorescence changes for GCaMP-M12 co-expressed with nt-M12 after employing siRNA for Orai1 (siOrai1). In siOrai1 treatment, increases in GCaMP-M12 fluorescence were delayed, and the degree of fluorescence increase was reduced (Figs. 2D-2G). To prove protein interactions between MS4A12 and Orai1, immunoprecipitation experiments were performed, in doings so, we found that GCaMP-M12 indeed interacted with Flag-Orai1 and that their interaction was enhanced upon thapsigargin treatment. Moreover, GCaMP-M12 and Orai1 interactions were confirmed by live cell imaging using GCaMP-M12 and mCherry-Orai1 expressed HEK cells (Fig. 2H). Therein, both proteins co-localized at the plasma membrane, and their co-localization was enhanced by thapsigargin treatment (Fig. 2I). Altogether, these results demonstrated that MS4A12 complexes with Orai1 and that the Ca^{2+} influx activity of MS4A12 is dependent on Orai1.

STIM1 co-expression decreases and STIM1 knockdown increases thapsigargin-induced increases in GCaMP-M12 fluorescence

Next, we examined the effects of STIM1on the SOCE-like behaviour of MS4A12. To do so, GCaMP-M12 with nt-M12 expressing cells were co-expressed with STIM1 via pIRES2 DsRED vector (expresses STIM1 and DsRED fluorescent proteins separately) to distinguish between STIM1-expressing red fluorescent cells (yellow dotted line cells, Fig. 3A) and non-expressing non-fluorescent cells (white dotted line cells, Fig. 3A). Cells expressing STIM1 showed significantly reduced changes in GCaMP-M12 fluorescence(Figs. 3B and 3C), compared to cells not expressing STIM1 (white dotted line cells, Figs. 3D). Meanwhile, when STIM1 expression was decreased with siRNA against STIM1 (siSTIM1), the fluorescence of GCaMP-M12 complexed with nt-M12 was more intense (Figs. 3D-3G). This was an unexpected and very compelling result, and implied that Ca^{2+} influx through MS4A12 is inhibited by STIM1 co-expression. In immunoprecipitation experiments, Flag-MS4A12 with myc-STIM1 showed protein interaction in normal conditions, and this interaction was slightly enhanced by thapsigargin (Fig. 3H). In addition, immunoprecipitation using each truncated protein showed that the cytosolic C terminal region (amino acids 225 to 267) of MS4A12 interacts with the CCD2+3, C2+3 region of STIM1 (STIM1-Orai activating region [SOAR] of STIM1) (Figs. 3I and 3J, Supplementary Fig. S2). Next, to examine the effect of Orai1 on the binding of $STIM1^{D76A}$ (constitutive active form) with MS4A12, Orai1 was over-expressed, and the binding strength of $STIM1^{D76A}$ with MS4A12 was observed (Fig. 3K). Interestingly, MS4A12 binding to $STIM1^{D76A}$ was reduced by Orai1 over-expression. These results indicated that STIM1 might face competitive in the presence of Orai1. Immunostaining for MS4A12 and STIM1 revealed that these two proteins are closely localised at some region and that, even in a normal state, thapsigargin treatment did not elicit big large changes in their co-localization (Fig. 3L). Overall, these data suggested that MS4A12 is not a canonical SOCE channel directly regulated by STIM1, because Ca^{2+} influx through MS4A12 is inhibited by STIM1 and because MS4A12 binding to $STIM1^{D76A}$ is inhibited by Orai1 over-expression.

Apical expression of MS4A12 in human colonic crypts and polarised T84 cells decreases in colon cancer malignancy

The expression of MS4A12 in colon cancer is controversial (Dalerba et al., 2011; Drew et al., 2014; Koslowski et al., 2008). We compared the expression levels of MS4A12 and Orai1 in samples from patients with colon cancer and colon cancer cell lines using RT-PCR and quantitative PCR (Figs. 4A and 4B). H508, CaCO-2, and HT29 cells, human adenocarcinoma cell lines originating from the colon, were used to examine mRNA expression levels of MS4A12. A549 cells, a human adenocarcinoma originating from the lung, was used as a negative control of MS4A12 expression. All three colon cancer cell lines, as well as A549 cells, showed no MS4A12 mRNA expression, whereas Orai1 showed high mRNA expression. In addition, MS4A12 expression was significantly lower in the cancer tissue than normal tissue (margins of colon cancers) from surgically removed specimens from colon cancers patient (described in Supplementary Table S1), which indicated that the expression of MS4A12 decreases during cancerous transformation. Moreover, we examined protein integrity and expression levels in normal and cancer tissue lysates (Fig. 4C). MS4A12 protein was clearly observed in normal colon tissue lysates, but significantly decreased in cancer tissue lysates. Accordingly, we deemed that protein and mRNA expression of MS4A12 is decreased in cancer states of the human colon and that MS4A12 expression is normal in the human colon protein, not a colon cancer marker.

DISCUSSION

MS4A12 was reported as a store-operated Ca^{2+} channel (Koslowski et al., 2008). However, no studies have examined the specific molecular mechanisms of the store-operated Ca^{2+} channel function of MS4A12. Our study demonstrated that the store-operated Ca^{2+} influx activity of MS4A12 is driven by a hetero-complex formed by MS4A12 and Orai1. The plasma membrane localization of GCaMP-M12 by co-expression of nt-MS4A12 or flag-Orai1 indicates that the hydrophobicity required for the membrane insertion is achieved by homo (with nt-M12; Fig. 1A)- or hetero (with Flag-Orai1; Figs. 2A and 2B)-complex formation with GCaMP-M12. Immunoprecipitation and co-localization of MS4A12 and Orai1 confirmed that MS4A12 interacts with Orai1 and that their interaction is further enhanced by thapsigargin (Figs. 2H and 2I). Interestingly,

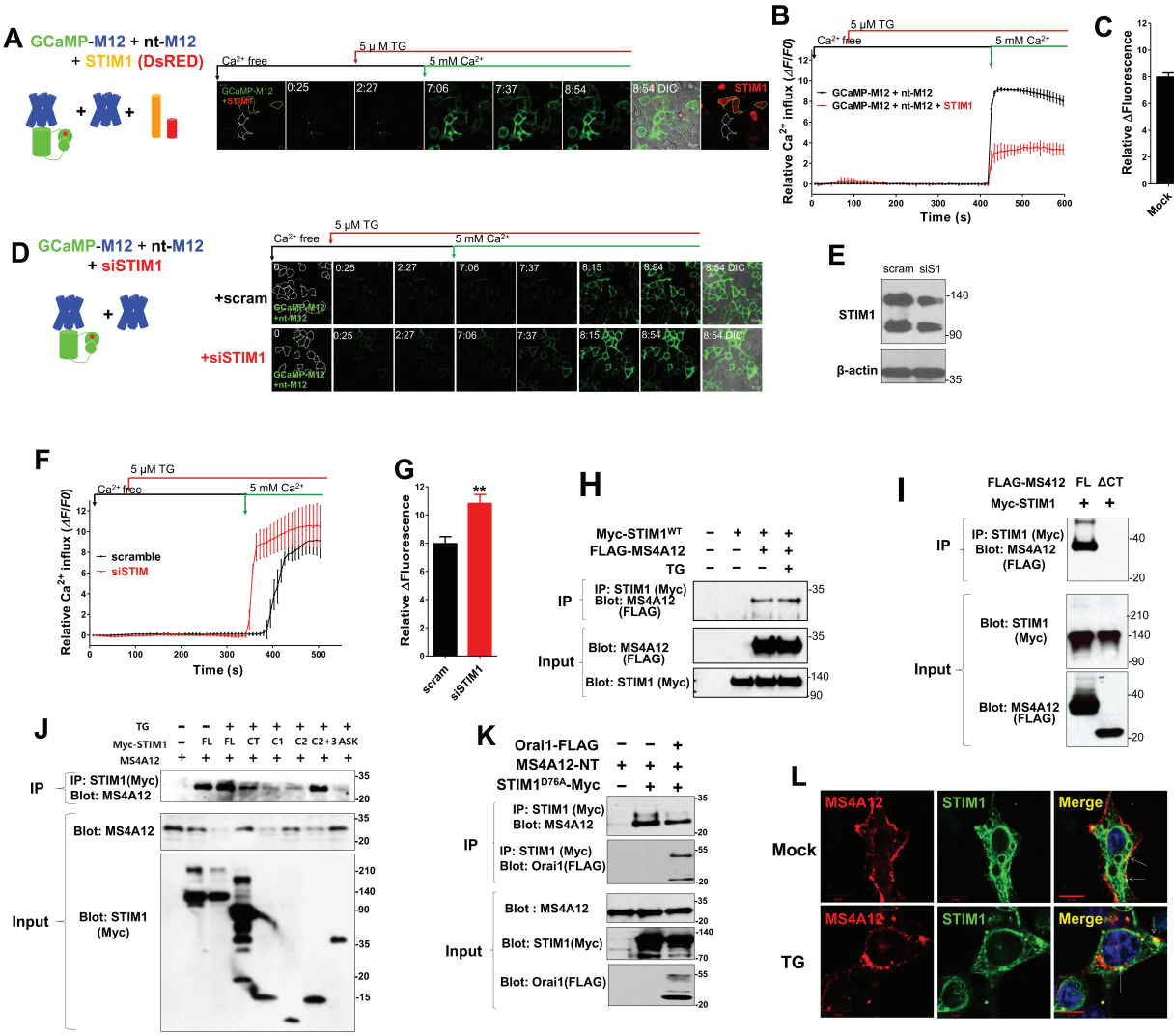

Fig. 3. STIM1 overexpression inhibits thapsigargin (TG)- and Ca^{2+}-dependent increases in GCaMP-M12 fluorescence, and interaction between MS4A12 and STIM1 are reduced by Orai1. (A-C) Thapsigargin- and Ca^{2+}-dependent fluorescence changes GCaMP-M12 (co-expressed with nt-M12) in a STIM1 overexpressed condition. (A) Images at each indicated time point. STIM1 co-expressed cells are indicated by yellow dotted lines, and non-STIM1-expressing cells are indicated by white dotted lines. (B) Traces of fluorescence changes. Summary is in (C). $***P \leq 0.001$. (D-G) Thapsigargin- and Ca^{2+}-dependent fluorescence changes in GCaMP-M12 (with nt-M12) under a STIM1 knockdown condition. siRNA efficiency for STIM1 was confirmed by Western blot with STIM1-specific antibody. (F) The fluorescence change traces. Summary is in (G). $**P \leq 0.01$. (H) MS4A12 whole protein interaction with $STIM1^{WT}$ in normal and thapsigargin-treated conditions. (I) Truncated MS4A12, in which the intracellular c-terminal region was deleted, shows failed protein-protein interaction with STIM1. (J) Truncated STIM1 proteins were used to detect the MS4A12 interacting region of STIM1. (K) MS4A12 interaction with $STIM1^{D76A}$ was decreased by Orai1 over-expression, while $STIM1^{D76A}$ interacted with Orai1. (L) MS4A12 (red) and STIM1 (green) localization in normal and thapsigargin conditions of HEK293 cells analyzed by immunostaining. White arrows indicate their co-localized region. Scale bars = 10 μm.

STIM1 co-expression inhibited thapsigargin-activated increases in fluorescence for GCaMP-M12 complexed with nt-M12 (Figs. 3A-3G), and this was recovered by siSTIM1 treatment. In addition, Flag-Orai1 co-expression decreased MS4A12 protein interactions with STIM1 (Fig. 3K). Altogether, these data imply that MS4A12 contributes to store-operated Ca^{2+} influx via complex formation with Orai1. However, given the inhibited store-operated Ca^{2+} influx upon STIM1 over-expression, MS4A12 seems to be a non-canonical component protein for store-operated Ca^{2+} influx.

The characteristic of MS4A12 as a store-operated Ca^{2+} channel only when it forms a hetero-complex with Orai1 is similar to that of TRPC3, which store-operated Ca^{2+} influx activity dependent on TRPC1 (Yuan et al., 2007). However, TRPC3 does not bind to STIM1 directly. In this regard, the relationship between MS4A12 and STIM1 is different from

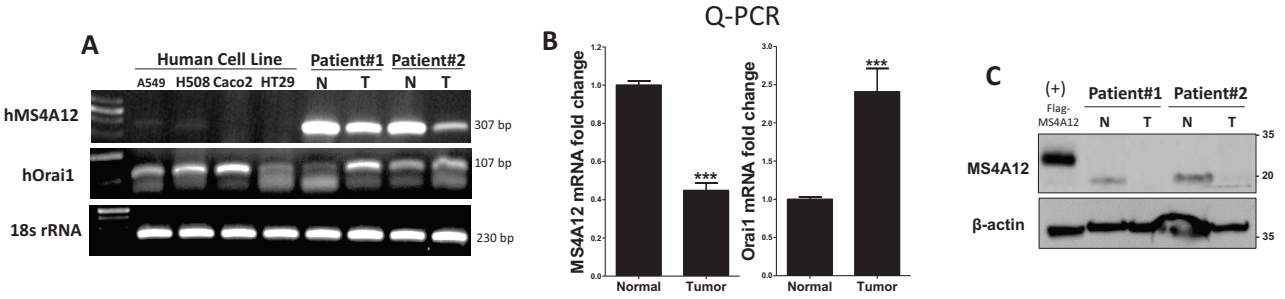

Fig. 4. Decreased mRNA and protein expression of MS4A12 in colon cancer. (A) mRNA expression of hMS4A12 and hOrai1 in normal and tumour tissue from patients with colon cancer and a human colon cancer cell line. 18s rRNA expression to indicate cDNA levels and integrity in each sample. N indicates normal and T indicates tumour regions of colon specimens. (B) Decreased hMS4A12 and increased hOrai1 mRNA expression in cancer tissue analysed by quantitative PCR (Q-PCR). ***$P \leq 0.001$ compared to normal. (C) Protein expression of MS4A12 in normal and cancer tissues. Actin was used as a loading control. Flag-MS4A12 plasmid expressing HEK lysate was used as a positive control for Western blotting.

that between TRPC3 and STIM1, in that MS4A12 can bind to STIM1, but their binding is competitively inhibited by Orai1. Additional observations are necessary to determine the physiological situation in which MS4A12 forms a hetero-complex with Orai1.

The locations of MS4A12, STIM1, and Orai1 appear to differ in cancer tissue and normal tissue (Supplementary Fig. S2). The apical major localization of MS4A12 in normal colon tissue (Supplementary Fig. S2A) was not observed in cancer tissues (Supplementary Fig. S2B). In addition, STIM1 and Orai1 localization changed in cancer tissue. Most of all, in cancer tissue, MS4A12 was nearly completely diminished, as seen in Western blot analysis (Fig. 4C). Considering the contribution of aberrant ion channel localization during cancer progression, such as $Ca_{V1.2}$ in colon cancer (Wang et al., 2000) and TRPM8 in prostate cancer (Monteith et al., 2007; Thebault et al., 2005), the altered location of Orai1 and STIM1, as well as the disappearance of MS4A12, may contribute to cancer progression.

Given that anti-CD20 monoclonal antibodies are effective immune-therapeutics for human malignancies, other MS4A family members have been identified as potential targets for therapeutic intervention (Koslowski et al., 2008; Liang and Tedder, 2001). However, MS4A12 is unlikely to be useful as a colon cancer-specific target for cancer immunotherapy because its expression is mostly eradicated during cancer transformation (Fig. 4). Whether MS4A12 can be used as a colon cancer immunotherapy target with Ca^{2+} influx function should be reconsidered. Rather, the decreased expression of MS4A12 may be a marker of poor prognosis (Dalerba et al., 2011; Drew et al., 2014). Based on our results showing reduced expression in cancer tissues, it is necessary to further investigate the role of MS4A12 under normal colon conditions and the effect of decreased MS4A12 expression on the malignant processes of colon cancer. In the meantime, we have identified another colon-expressed MS4A member, MS4A8, that shows increased expression upon cancer transition. However, this protein does not appear to be expressed in the plasma membrane according to immunocytochemistry data using MS4A8 over-expressing cells and live cell imaging of mCherry tagged-MS4A8 (Supplementary Fig. S3).

In conclusion, we suggest that MS4A12 is not a STIM1-regulated canonical store-operated Ca^{2+} influx channel and shows store-operated Ca^{2+} influx activity when it forms a hetero-complex with Orai1. Additionally, our results indicate that MS4A12 is a colon protein marker and that its expression is decreased during cancerous states.

Note: Supplementary information is available on the Molecules and Cells website (www.molcells.org).

ACKNOWLEDGMENTS

This study was supported by a Korean government grant NFR-2019R1A2C1086348 and a faculty research grant from Yonsei University College of Medicine (4-2016-0600) for J.Y.K.

AUTHOR CONTRIBUTIONS

J.Y.K. and M.J. conceived of and designed the experiments. J.W.H. performed the most of the experiments. W.H., D.L., H.Y.K., and I.J. performed IP experiments. W.H. and C.K. performed live imaging experiment using GCaMP-MS4A12. H.H. and M.J. contributed the materials from patients. J.Y.K. and J.W.H. analysed the data. I.S. and M.G.L. participated in design experiments and contributed reagents, materials and instruments. J.Y.K. wrote the manuscripts. All authors read and approved the final manuscript.

CONFLICT OF INTEREST

The authors have no potential conflicts of interest to disclose.

ORCID

Jung Woo Han https://orcid.org/0000-0002-8279-593X
Woon Heo https://orcid.org/0000-0001-8208-484X
Donghyuk Lee https://orcid.org/0000-0002-0045-5027
Choeun Kang https://orcid.org/0000-0001-7800-187X
Hye-Yeon Kim https://orcid.org/0000-0001-9095-0736
Ikhyun Jun https://orcid.org/0000-0002-2160-1679
Insuk So https://orcid.org/0000-0003-2294-2050
Hyuk Hur https://orcid.org/0000-0002-9864-7229

Min Goo Lee https://orcid.org/0000-0001-7436-012X
Minkyu Jung https://orcid.org/0000-0001-8281-3387
Joo Young Kim https://orcid.org/0000-0003-2623-1491

REFERENCES

Akerboom, J., Carreras Calderon, N., Tian, L., Wabnig, S., Prigge, M., Tolo, J., Gordus, A., Orger, M.B., Severi, K.E., Macklin, J.J., et al. (2013). Genetically encoded calcium indicators for multi-color neural activity imaging and combination with optogenetics. Front. Mol. Neurosci. *6,* 2.

Beers, S.A., Chan, C.H.T., French, R.R., Cragg, M.S., and Glennie, M.J. (2010). CD20 as a target for therapeutic type I and II monoclonal antibodies. Semin. Hematol. *47,* 107-114.

Bubien, J.K., Zhou, L.J., Bell, P.D., Frizzell, R.A., and Tedder, T.F. (1993). Transfection of the CD20 cell surface molecule into ectopic cell types generates a Ca2+ conductance found constitutively in B lymphocytes. J. Cell Biol. *121,* 1121-1132.

Dalerba, P., Kalisky, T., Sahoo, D., Rajendran, P.S., Rothenberg, M.E., Leyrat, A.A., Sim, S., Okamoto, J., Johnston, D.M., Qian, D., et al. (2011). Single-cell dissection of transcriptional heterogeneity in human colon tumors. Nat. Biotechnol. *29,* 1120-1127.

Drew, J.E., Farquharson, A.J., Mayer, C.D., Vase, H.F., Coates, P.J., Steele, R.J., and Carey, F.A. (2014). Predictive gene signatures: molecular markers distinguishing colon adenomatous polyp and carcinoma. PLoS One *9,* e113071.

Dynes, J.L., Amcheslavsky, A., and Cahalan, M.D. (2016). Genetically targeted single-channel optical recording reveals multiple Orai1 gating states and oscillations in calcium influx. Proc. Natl. Acad. Sci. U. S. A. *113,* 440-445.

Feske, S., Gwack, Y., Prakriya, M., Srikanth, S., Puppel, S.H., Tanasa, B., Hogan, P.G., Lewis, R.S., Daly, M., and Rao, A. (2006). A mutation in Orai1 causes immune deficiency by abrogating CRAC channel function. Nature *441,* 179-185.

Herter, S., Herting, F., Mundigl, O., Waldhauer, I., Weinzierl, T., Fauti, T., Muth, G., Ziegler-Landesberger, D., Van Puijenbroek, E., Lang, S., et al. (2013). Preclinical activity of the type II CD20 antibody GA101 (obinutuzumab) compared with rituximab and ofatumumab in vitro and in xenograft models. Mol. Cancer Ther. *12,* 2031-2042.

Kim, J.Y. and Muallem, S. (2011). Unlocking SOAR releases STIM. EMBO J. *30,* 1673-1675.

Ko, J., Myeong, J., Yang, D., and So, I. (2017). Calcium permeability of transient receptor potential canonical (TRPC) 4 channels measured by TRPC4-GCaMP6s. Korean J. Physiol. Pharmacol. *21,* 133-140.

Koslowski, M., Sahin, U., Dhaene, K., Huber, C., and Tureci, O. (2008). MS4A12 is a colon-selective store-operated calcium channel promoting malignant cell processes. Cancer Res. *68,* 3458-3466.

Li, H., Ayer, L.M., Lytton, J., and Deans, J.P. (2003). Store-operated cation entry mediated by CD20 in membrane rafts. J. Biol. Chem. *278,* 42427-42434.

Liang, Y. and Tedder, T.F. (2001). Identification of a CD20-, FcεRIβ-, and HTm4-related gene family: sixteen new MS4A family members expressed in human and mouse. Genomics *72,* 119-127.

Monteith, G.R., McAndrew, D., Faddy, H.M., and Roberts-Thomson, S.J. (2007). Calcium and cancer: targeting Ca2+ transport. Nat. Rev. Cancer *7,* 519-530.

Nguyen, L.P., Nguyen, H.T., Yong, H.J., Reyes-Alcaraz, A., Lee, Y.N., Park, H.K., Na, Y.H., Lee, C.S., Ham, B.J., Seong, J.Y., et al. (2020). Establishment of a NanoBiT-based cytosolic Ca(2+) sensor by optimizing calmodulin-binding motif and protein expression levels. Mol. Cells *43,* 909-920.

Ong, H.L., Cheng, K.T., Liu, X., Bandyopadhyay, B.C., Paria, B.C., Soboloff, J., Pani, B., Gwack, Y., Srikanth, S., Singh, B.B., et al. (2007). Dynamic assembly of TRPC1-STIM1-Orai1 ternary complex is involved in store-operated calcium influx. Evidence for similarities in store-operated and calcium release-activated calcium channel components. J. Biol. Chem. *282,* 9105-9116.

Parekh, A.B. (2010). Store-operated CRAC channels: function in health and disease. Nat. Rev. Drug Discov. *9,* 399-410.

Park, C.Y., Shcheglovitov, A., and Dolmetsch, R. (2010). The CRAC channel activator STIM1 binds and inhibits L-type voltage-gated calcium channels. Science *330,* 101-105.

Prakriya, M. and Lewis, R.S. (2015). Store-operated calcium channels. Physiol. Rev. *95,* 1383-1436.

Reff, M.E., Carner, K., Chambers, K.S., Chinn, P.C., Leonard, J.E., Raab, R., Newman, R.A., Hanna, N., and Anderson, D.R. (1994). Depletion of B cells in vivo by a chimeric mouse human monoclonal antibody to CD20. Blood *83,* 435-445.

Roberts, D.L., O'Dwyer, S.T., Stern, P.L., and Renehan, A.G. (2015). Global gene expression in pseudomyxoma peritonei, with parallel development of two immortalized cell lines. Oncotarget *6,* 10786-10800.

Roderick, H.L. and Cook, S.J. (2008). Ca2+ signalling checkpoints in cancer: remodelling Ca2+ for cancer cell proliferation and survival. Nat. Rev. Cancer *8,* 361-375.

Rogers, L.M., Veeramani, S., and Weiner, G.J. (2014). Complement in monoclonal antibody therapy of cancer. Immunol. Res. *59,* 203-210.

Sabourin, J., Le Gal, L., Saurwein, L., Haefliger, J.A., Raddatz, E., and Allagnat, F. (2015). Store-operated Ca2+ entry mediated by Orai1 and TRPC1 participates to insulin secretion in rat beta-Cells. J. Biol. Chem. *290,* 30530-30539.

Shen, D., Wang, X., Li, X., Zhang, X., Yao, Z., Dibble, S., Dong, X.P., Yu, T., Lieberman, A.P., Showalter, H.D., et al. (2012). Lipid storage disorders block lysosomal trafficking by inhibiting a TRP channel and lysosomal calcium release. Nat. Commun. *3,* 731.

Sobradillo, D., Hernandez-Morales, M., Ubierna, D., Moyer, M.P., Nunez, L., and Villalobos, C. (2014). A reciprocal shift in transient receptor potential channel 1 (TRPC1) and stromal interaction molecule 2 (STIM2) contributes to Ca2+ remodeling and cancer hallmarks in colorectal carcinoma cells. J. Biol. Chem. *289,* 28765-28782.

Thebault, S., Lemonnier, L., Bidaux, G., Flourakis, M., Bavencoffe, A., Gordienko, D., Roudbaraki, M., Delcourt, P., Panchin, Y., Shuba, Y., et al. (2005). Novel role of cold/menthol-sensitive transient receptor potential melastatine family member 8 (TRPM8) in the activation of store-operated channels in LNCaP human prostate cancer epithelial cells. J. Biol. Chem. *280,* 39423-39435.

Vacher, P., Vacher, A.M., Pineau, R., Latour, S., Soubeyran, I., Pangault, C., Tarte, K., Soubeyran, P., Ducret, T., and Bresson-Bepoldin, L. (2015). Localized store-operated calcium influx represses CD95-dependent apoptotic effects of rituximab in non-Hodgkin B lymphomas. J. Immunol. *195,* 2207-2215.

Villalobos, C., Sobradillo, D., Hernandez-Morales, M., and Nunez, L. (2017). Calcium remodeling in colorectal cancer. Biochim. Biophys. Acta. Mol. Cell Res. *1864,* 843-849.

Walshe, C.A., Beers, S.A., French, R.R., Chan, C.H.T., Johnson, P.W., Packham, G.K., Glennie, M.J., and Cragg, M.S. (2008). Induction of cytosolic calcium flux by CD20 is dependent upon B cell antigen receptor signaling. J. Biol. Chem. *283,* 16971-16984.

Wang, X.T., Nagaba, Y., Cross, H.S., Wrba, F., Zhang, L., and Guggino, S.E. (2000). The mRNA of L-type calcium channel elevated in colon cancer: protein distribution in normal and cancerous colon. Am. J. Pathol. *157,* 1549-1562.

Wang, Y., Deng, X., Mancarella, S., Hendron, E., Eguchi, S., Soboloff, J., Tang, X.D., and Gill, D.L. (2010). The calcium store sensor, STIM1, reciprocally controls Orai and CaV1.2 channels. Science *330,* 105-109.

Yuan, J.P., Zeng, W., Huang, G.N., Worley, P.F., and Muallem, S. (2007). STIM1 heteromultimerizes TRPC channels to determine their function as store-operated channels. Nat. Cell Biol. *9,* 636-645.

Zuccolo, J., Bau, J., Childs, S.J., Goss, G.G., Sensen, C.W., and Deans, J.P. (2010). Phylogenetic analysis of the MS4A and TMEM176 gene families. PLoS One *5,* e9369.

Zuccolo, J., Deng, L., Unruh, T.L., Sanyal, R., Bau, J.A., Storek, J., Demetrick, D.J., Luider, J.M., Auer-Grzesiak, I.A., Mansoor, A., et al. (2013). Expression of MS4A and TMEM176 genes in human B lymphocytes. Front. Immunol. *4,* 195.